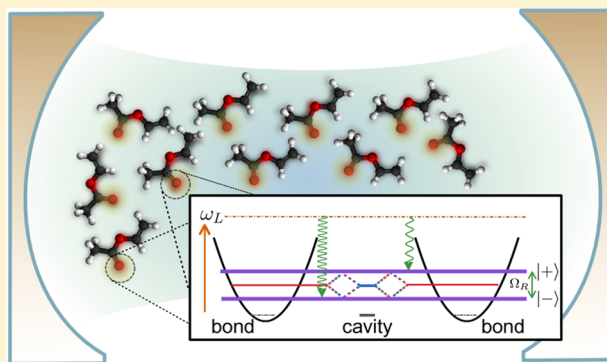


Signatures of Vibrational Strong Coupling in Raman Scattering

Javier del Pino,^{*,†} Johannes Feist,^{*,†} and F. J. Garcia-Vidal^{*,†,‡}[†]Departamento de Física Teórica de la Materia Condensada and Condensed Matter Physics Center (IFIMAC), Universidad Autónoma de Madrid, Madrid E-28049, Spain[‡]Donostia International Physics Center (DIPC), E-20018 Donostia/San Sebastian, Spain

ABSTRACT: We have analyzed theoretically how the emergence of collective strong coupling between vibrational excitations and confined cavity modes affects Raman scattering processes. This work was motivated by recent experiments (Shalabney et al. *Angew. Chem., Int. Ed.* **2015**, *54*, 7971) that reported enhancements of up to 3 orders of magnitude in the Raman signal. By using different models within linear response theory, we show that the total Raman cross section is maintained constant when the system evolves from the weak-coupling limit to the strong-coupling regime. A redistribution of the Raman signal among the two polaritons is the main fingerprint of vibrational strong coupling in the Raman spectrum.



Raman scattering is one of the principal methods used to obtain information about material properties and chemical structures.¹ In particular, it probes the rovibrational structure of matter and can thus be used to provide a “fingerprint”, making it useful for a wide range of applications in research and industry. Its operating principle relies on the inelastic scattering of optical photons (frequency ω_L), which leads to the emission of photons at shifted frequencies $\omega_L - \delta\omega$. The observed frequency shifts $\delta\omega$ correspond to Raman-allowed excitations in the system under study and thus provide detailed information about its (rovibrational) states. Vibrational excitations are often well-approximated by harmonic oscillators, leading to a series of equidistant Stokes lines $\delta\omega = n\omega_v$ for each mode, corresponding to the excitation of n vibrational quanta.

Recently, it was shown that vibrational excitations interacting with confined cavity modes can enter the vibrational-strong-coupling (VSC) regime.^{2–6} Strong coupling, already well-known in the context of electronic excitations (see refs 7 and 8 for recent reviews), occurs when the coherent energy exchange between a light mode and matter excitations is faster than the decay and/or decoherence of either constituent. The fundamental excitations of the two systems then become inextricably linked and can be described as hybrid light–matter quasi-particles, so-called polaritons, that combine the properties of both constituents. Consequently, the vibro-polaritons obtained under VSC are formed by superpositions of a cavity photon and excited molecular bond vibrations that are collectively distributed over a large number of molecules.

A recent pioneering experiment⁹ measured spontaneous Raman scattering under collective strong coupling of the (IR- and Raman-active) C=O bond of a polymer (polyvinyl acetate, PVAc) to Fabry–Perot cavity photons. A large increase of the Raman signal under strong coupling was observed, with emission at energy shifts $\delta\omega$ approximately corresponding to

the upper and lower polaritons. This intriguing result motivated our current study. We have theoretically investigated the signatures of vibrational strong coupling in the Raman spectrum. In this phenomenon, the vibrational excitation is modified by interaction with the cavity. In contrast to the well-known technique of surface-enhanced Raman scattering,^{10–12} in which plasmonic modes enhance the optical transitions (absorption and emission) directly, the thin metallic mirrors used in the experimental setup of Shalabney et al. do not efficiently confine light at optical wavelengths, and the optical transitions are almost unmodified.⁹ As opposed to surface-enhanced Raman scattering, there is no known simple picture that explains a possible enhancement of the Raman cross section under vibrational strong coupling. Additionally, vibrational-pumping effects such as recently found for SERS within a quantized model¹³ do not play a role here either.

In Raman scattering, a driving laser beam induces an oscillating polarization in a molecule, which then couples to the polarization of a vibrational transition of either higher (Stokes) or lower (anti-Stokes) energy, leading to emission of photons shifted by the vibrational energy. Figure 1 illustrates this inelastic scattering process for the first Stokes line of a single molecular vibration, in both the weak- and strong-coupling regimes. As a minimal model to reproduce this phenomenon, in our first approach, we restrict the description of the bare molecules to a three-level system consisting of the ground state, $|g\rangle$, with energy ω_g , the first excited vibrational mode, $|v\rangle$, with energy ω_v , and the electronically excited state, $|e\rangle$, with energy ω_e . Additionally, we include a quantized cavity mode, which, within the minimal model, we restrict to containing at

Received: November 29, 2015

Revised: December 8, 2015

Published: December 8, 2015

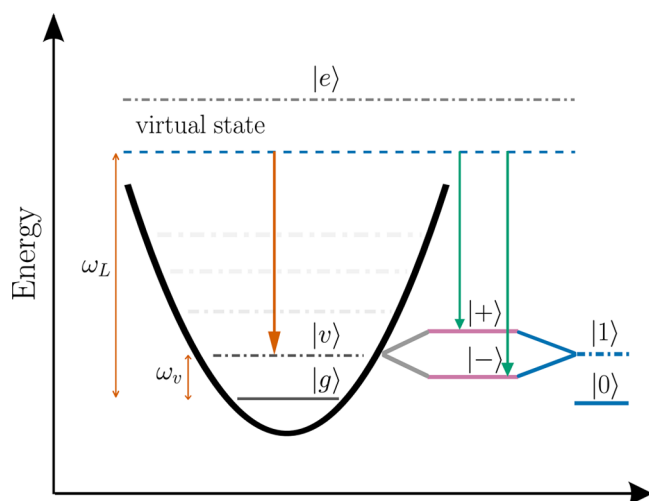


Figure 1. Schematic of the Raman scattering process for a molecule as a result of excitation with an off-resonant driving field. After coherent excitation, the molecule is promoted to a virtual state, depicted as a blue dashed line. In the weak-coupling regime, the electron decays into the first excited vibrational state, $|v\rangle$ (orange arrow). When this first excited vibrational state is strongly coupled to the cavity mode, $|1\rangle$, the electron can decay to either of the two polaritons, $|+\rangle$ or $|-\rangle$ (blue arrows).

most a single photon, $|1\rangle$, with energy ω_c . In all of the calculations presented in this work, we consider the case of zero detuning, that is, $\omega_c = \omega_v$. Choosing ω_g as the zero energy, the coherent dynamics of the system composed of N molecules and a cavity mode is governed by the Hamiltonian ($\hbar = 1$)

$$\hat{H} = \omega_c |1\rangle\langle 1| + \sum_{i=1}^N [\omega_v |v_i\rangle\langle v_i| + \omega_e |e_i\rangle\langle e_i| + g(|1\rangle\langle v_i| + |v_i\rangle\langle 1|)] \quad (1)$$

where the cavity–oscillator interaction is measured by g , which depends on the cavity electric field strength and the change of the molecular dipole moment under displacement from the equilibrium position but, in our calculations, will be used as a parameter that fixes the Rabi splitting (see below). For simplicity, we assume a configuration with zero disorder in which all N molecules are equally coupled to the cavity mode. We verified that this assumption does not affect the conclusions presented here. We note here that, in contrast to our previous work on VSC,⁵ the Hamiltonian includes an electronically excited state that allows for the description of the inelastic scattering of optical photons.

We assume that the probe field is far off-resonant and that the hierarchy condition $\omega_v \ll \omega_L \ll \omega_e$ is fulfilled. We can then safely work within second-order perturbation theory and neglect losses in the system. In general, the Raman scattering cross section associated with a process in which the system is excited from the initial state $|i\rangle$ (energy ω_i) to a final state $|f\rangle$ (energy ω_f) with scattered photon energy $\omega_L - \omega_f + \omega_i$ can be written as $\sigma_{R,\omega_f-\omega_i} \propto |\alpha_{fi}|^2$, where

$$\alpha_{fi} = \langle f|\hat{\alpha}|i\rangle = \langle f|\hat{\mu} \frac{1}{\hat{H} - \omega_L - \omega_i} \hat{\mu}|i\rangle$$

is the polarizability matrix element between the initial and final states, $\hat{\mu}$ is the dipole operator. In our case, we consider only dipolar transitions $|g\rangle \rightarrow |e\rangle$, characterized by a dipole

moment μ_{ge} and $|e\rangle \rightarrow |v\rangle$ with dipole moment μ_{ev} corresponding to an electronic excitation from the ground state and transition from the electronically excited state to the first excited vibrational mode, respectively. For vibrational modes that are IR-active (as required for VSC), there are also direct dipole transitions from the ground state to the vibrationally excited state. However, these do not play a role in Raman scattering to the vibrationally excited modes, which requires two dipole transitions.

In the weak-coupling regime ($g \rightarrow 0$), the Raman scattering process corresponds to an excitation from the global ground state, $|G\rangle = \prod_{i=1}^N |g_i\rangle$, followed by decay into a singly excited vibrational state of a molecule, $|v\rangle_i$ (shorthand for $|v\rangle_i \prod_{j \neq i} |g_j\rangle$), with index $i = 1, \dots, N$ labeling different molecules. In this situation, the molecules act independently, and the cross section for emission of a photon of energy $\omega_L - \omega_v$ is just the sum of the cross sections associated with each molecule

$$\sigma_{R,\omega_v} \propto \sum_{i=1}^N |\alpha_{v_i G}|^2 = N \left(\frac{\mu_{ve} \mu_{ge}}{\omega_e - \omega_L} \right)^2 \quad (2)$$

In the VSC regime, the $(N + 1)$ singly excited eigenstates of the system are formed by (i) two polaritons

$$|\pm\rangle = \frac{1}{\sqrt{2}}(|1\rangle \pm |B\rangle)$$

which are symmetric and antisymmetric linear combinations of the cavity mode, $|1\rangle$, with the collective bright state of the molecular excitation

$$|B\rangle = \frac{1}{\sqrt{N}} \sum_{i=1}^N |v_i\rangle$$

and (ii) the so-called dark states, $|d\rangle$, $(N - 1)$ combinations of molecular excitations orthogonal to $|B\rangle$ that have eigenfrequencies ω_v and no electromagnetic component. The eigenfrequencies of the two polariton modes are $\omega_{\pm} = \omega_v \pm g\sqrt{N}$, the Rabi splitting being $\Omega_R = 2g\sqrt{N}$. In principle, it could be expected that the formation of collective modes among the molecular bonds leads to an enhancement of the Raman cross section. However, a straightforward calculation shows that the Raman cross sections associated with the dark modes are zero whereas those of the two polaritons (involving photons of energies $\omega_L - \omega_+$ and $\omega_L - \omega_-$) are just one-half of the Raman cross section evaluated in the weak-coupling limit (eq 2). In other words, when going from the weak- to the strong-coupling regime, the total Raman cross section is maintained but equally shared between the two polaritons.

This is an interesting result, as it points to the existence of a kind of sum rule for the Raman scattering cross section. To investigate this issue in more detail, we analyze the total Raman scattering cross section defined as the sum over all possible final states, $|f\rangle$, resulting from inelastic processes when the system is excited from the ground state $|G\rangle$

$$\Sigma_R \propto \sum_{f \neq G} |\langle f|\hat{\alpha}|G\rangle|^2 = \langle G|\hat{\alpha}^2|G\rangle - \langle G|\hat{\alpha}|G\rangle^2 \quad (3)$$

where we have used the closure relation $\sum_{f \neq G} |f\rangle\langle f| = \hat{I} - |G\rangle\langle G|$. This result is related to general sum rules in linear response theory that have been investigated, for example, in the context of Raman scattering from strongly correlated systems.^{14–16} Here, we are interested in the change

of the cross section as the Hamiltonian is changed and VSC is established. By inserting the spectral decomposition of the Hamiltonian in

$$\hat{\alpha} = \hat{\mu} \frac{1}{\hat{H} - \omega_L - \omega_i} \hat{\mu}$$

it can be seen that the total Raman cross section will only be affected by changes in the ground state $|G\rangle$ or intermediate electronically excited states $|n\rangle$ reachable by a single-photon transition, $\langle n|\hat{\mu}|G\rangle \neq 0$. Vibrational strong coupling primarily affects the final states, that is, the vibrationally excited states that split into polaritons. Furthermore, as the driving frequency ω_L in standard Raman scattering experiments is not close to any eigenstate of the Hamiltonian, any possible changes in the electronically excited states are not expected to have a significant effect. This suggests that, within the theoretical framework described above, changes in the total Raman cross section when going from the weak-coupling limit to the strong-coupling regime could come only from changes in the ground state of the system. Such changes are induced by the counter-rotating terms in the cavity–emitter coupling, which become important in the so-called ultrastrong-coupling regime, reached when the Rabi frequency Ω_R is a non-negligible fraction of the transition energy ω_v .^{17–21} The strength of these effects scales (to lowest order) as g^2 , such that the effects are small but nonzero even for small couplings. Furthermore, it has recently been shown that the changes induced in the ground state depend sensitively on the observable that is interrogated,^{22,23} with bond-length changes, for example, being sensitive only to the single-molecule coupling strength whereas energy shifts depend on the collective coupling. It is thus necessary to explicitly calculate whether counter-rotating terms could affect the ground state and enhance the Raman scattering cross section.

To check the formalism above, as well as go beyond it, we therefore turn to a microscopic quantum model for organic molecules interacting with the quantized cavity field. In this formalism, we include counter-rotating terms to explore the effects of ultrastrong coupling and additionally incorporate losses and dephasing mechanisms that were not present in the previous approach. The Hamiltonian describing the i th bare molecule now reads

$$\hat{H}_{\text{mol}}^{(i)} = \omega_e \hat{\sigma}_i^\dagger \hat{\sigma}_i + \omega_v [\hat{b}_i^\dagger \hat{b}_i + \sqrt{S} \hat{\sigma}_i^\dagger \hat{\sigma}_i (\hat{b}_i^\dagger + \hat{b}_i)] \quad (4)$$

where the electronic transition of the molecule, of energy ω_e , is described by the Pauli ladder operator $\hat{\sigma}_i$, whereas \hat{b}_i is the annihilation operator of the optically active vibrational mode of the molecule of energy ω_v . The interaction between electronic and vibrational states is characterized by the Huang–Rhys parameter S , which quantifies the phonon displacement between the ground and excited electronic states. The total Hamiltonian also contains the cavity field and the coupling term between the cavity mode and the vibrational states of the molecules

$$\hat{H} = \sum_{i=1}^N \hat{H}_{\text{mol}}^{(i)} + \omega_c \hat{a}^\dagger \hat{a} + g \sum_{i=1}^N (\hat{a} + \hat{a}^\dagger) (\hat{b}_i + \hat{b}_i^\dagger) \quad (5)$$

where \hat{a} is the annihilation operator for the cavity mode with energy ω_c . As in our previous approach above, g describes the cavity–vibrational mode interaction, but the Hamiltonian in eq 5 now includes counter-rotating terms that do not conserve

the number of excitations. We note that, in contrast to our previous work on VSC,⁵ the current model describes both electronic and vibrational degrees of freedom of the molecule, as well as their coupling, to allow for the description of the Raman scattering process. In addition, neither the photonic nor the vibrational degrees of freedom are restricted to the single-excitation subspace. Consequently, this theoretical framework permits the investigation of higher Stokes lines, corresponding to vibrational overtones. The photonic and vibrational degrees of freedom form a system of coupled harmonic oscillators that can be diagonalized analytically, yielding $N + 1$ new oscillator modes: the upper and lower polariton modes with frequencies $\omega_{\pm} = \omega_v \sqrt{1 \pm 2g/\omega_v}$, as well as $N - 1$ dark-state oscillators at the uncoupled frequencies ω_v .

To account for both loss and dephasing mechanisms, we rely on the standard Lindblad master-equation formalism.²⁴ We include decay of the electronic excitations (rate γ_e) and vibrational modes (rate γ_v), as well as the loss of the cavity photons (rate κ). Additionally, we consider elastic scattering with bath modes, which leads to pure electronic (rate γ_e^ϕ) and vibrational (rate γ_v^ϕ) dephasing terms. The time evolution of the density matrix $\hat{\rho}$ is then described by

$$\begin{aligned} \partial_t \hat{\rho} = & -i[\hat{H}, \hat{\rho}] + \kappa \mathcal{L}_a[\hat{\rho}] + \sum_{i=1}^N (\gamma_e \mathcal{L}_{\hat{\sigma}_i}[\hat{\rho}] + \gamma_v \mathcal{L}_{\hat{b}_i}[\hat{\rho}] \\ & + \gamma_e^\phi \mathcal{L}_{\hat{\sigma}_i^\dagger \hat{\sigma}_i}[\hat{\rho}] + \gamma_v^\phi \mathcal{L}_{\hat{b}_i^\dagger \hat{b}_i}[\hat{\rho}]) \end{aligned} \quad (6)$$

where $\mathcal{L}_{\hat{X}}[\hat{\rho}] = \hat{X} \hat{\rho} \hat{X}^\dagger - \frac{1}{2} \{ \hat{X}^\dagger \hat{X}, \hat{\rho} \}$. We note that, in the ultrastrong-coupling regime, the Hamiltonian does not conserve the number of excitations and the terms $\mathcal{L}_a[\hat{\rho}]$ and $\mathcal{L}_{\hat{b}_i}[\hat{\rho}]$ actually introduce artificial pumping. We then replace these terms by explicitly calculating the decay introduced by coupling to a zero-temperature bath of background modes with constant spectral density, within Bloch–Redfield–Wangsness (BRW) theory.^{25,26} As we previously showed,⁵ BRW theory should, in principle, also be used for the description of vibrational dephasing; however, this does not influence the results presented here significantly, and we thus use Lindblad terms for simplicity.

We additionally introduce a continuous-wave off-resonant laser field at frequency ω_L that collectively drives all emitters, represented by $\hat{H}_d = \Omega_p \sum_i (\hat{\sigma}_i e^{-i\omega_L t} + \hat{\sigma}_i^\dagger e^{i\omega_L t})$. The emission spectrum is then calculated from the steady-state two-time correlation function of the electronic dipole within a frame rotating at ω_L in which \hat{H}_d is time-independent. This gives the emission spectrum $S(\omega) = \int_{-\infty}^{\infty} e^{i(\omega_L - \omega)\tau} \langle \hat{\sigma}^\dagger(\tau) \hat{\sigma}(0) \rangle d\tau$, where $\hat{\sigma} = \sum_i \hat{\sigma}_i$, from which we remove the zero-frequency Rayleigh peak to obtain only the Raman contribution. For the numerical implementation of this microscopic model, we employ the open-source QuTiP package.²⁷

We first apply this theoretical framework to study the Raman spectrum when the vibrational mode of a single molecule is coupled to the cavity mode. The results are depicted in Figure 2, with parameters chosen to agree with experiment.⁹ The vibrational frequency is $\omega_v = 1730 \text{ cm}^{-1}$, and the vibrational rates, $\gamma_v = \gamma_v^\phi = 13 \text{ cm}^{-1}$, are recovered from the experimental transmission spectrum assuming that one-half of the total line width is due to pure dephasing. The cavity losses are taken into account by $\kappa = 13 \text{ cm}^{-1}$, which is a relatively small value chosen to make the separate peaks clearly visible. Other parameters are chosen in accordance with typical values for polymers: $\omega_e = 5 \text{ eV}$, $\omega_L \gg \omega_v$, $S = 2$, $\gamma_e = 50 \text{ cm}^{-1}$, and $\gamma_e^\phi = 50 \text{ cm}^{-1}$.

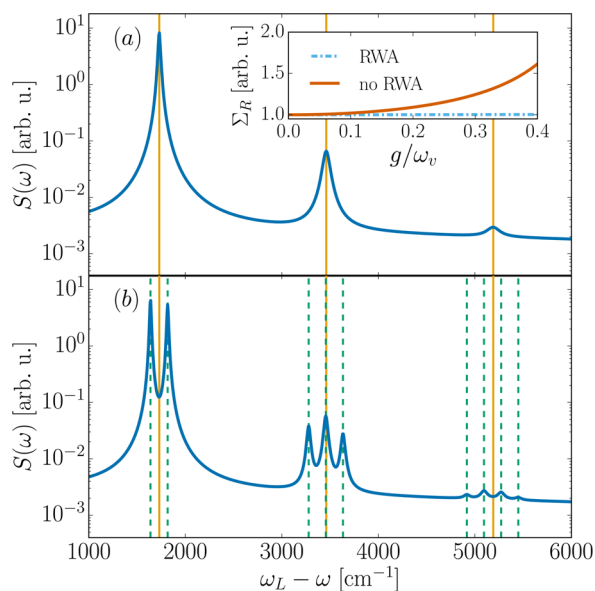


Figure 2. Single-molecule Raman spectra in the (a) weak- and (b) strong-coupling regimes. A weak probe strength $\Omega_p \ll \omega_v$ is used in both cases. The Stokes lines at energies $n\omega_v$, $n \in \mathbb{N}$, are depicted in orange, whereas the dashed green lines, spectrally located at $\omega^{(k,l)}$ (see main text), show the dressed energies in the strong-coupling regime. In this last calculation, we allowed for at most five excitations. Inset: Total Raman scattering probability $\int S(\omega) d\omega \propto \Sigma_R$ as a function of cavity–oscillator interaction g , with (blue) and without (orange) the rotating-wave approximation.

As expected, in the weak-coupling limit, namely, $g \rightarrow 0$ (Figure 2a), Stokes lines appear at the vibrational frequencies $n\omega_v$, with $n \in \mathbb{N}$. When VSC emerges ($\Omega_R = 160 \text{ cm}^{-1}$ in Figure 2b), the n th Stokes line splits into $n + 1$ sidebands at $\omega^{(k,l)} = k\omega_- + l\omega_+$ corresponding to the excitation of k lower and l upper polaritons, with $k + l = n$. Importantly, the positions of the $n = 1$ Stokes lines coincide with their positions in the transmission spectrum, and consequently, the splitting between the two peaks coincides with Ω_R , the Rabi splitting observed in the transmission spectrum. In addition, the total Raman signal $\int S(\omega) d\omega \propto \Sigma_R$ stays almost constant when going from the weak- to the strong-coupling regime. This result is compatible with the prediction obtained from the pure Hamiltonian approach (eq 3) and confirms the expectation that counter-rotating terms are negligible for the current case of $\Omega_R \ll \omega_v$.

To observe changes in the total Raman signal induced by the counter-rotating terms, we render the evolution of the total Raman scattering probability as a function of g , shown in the inset of Figure 2a) (with all other parameters being the same as those used in the main panels of Figure 2). These results demonstrate that, under ultrastrong coupling, the total Raman cross section could indeed change significantly, as it increases by a factor of more than 1.5 in the limit $g \rightarrow \omega_v/2$ (larger values of g are unphysical within this model). However, notice that, in the experiments by Shalabney et al.,⁹ $g/\omega_v \approx 0.05$, and our results show that the ground state is modified only weakly, leading to a total Raman scattering probability that is practically unchanged from the weak-coupling limit $g \rightarrow 0$.

Our previous results using the microscopic model were obtained for a single molecule. As a minimal model to investigate collective effects, we now show the Raman spectrum of two molecules strongly coupled to a cavity mode. For comparison with the single-molecule case, we rescale $g \rightarrow g/\sqrt{2}$ to

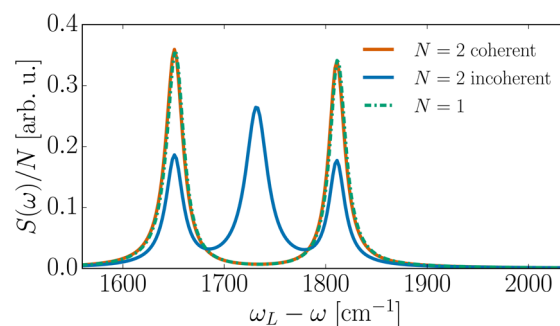


Figure 3. First Stokes lines of the Raman spectra in the strong-coupling regime for one and two molecules. The chosen parameters are the same as those used for the single-molecule case, with the spectra normalized to the number of molecules N . For the case of two molecules, the spectra for coherent and incoherent collections are depicted. For comparison, the case of a single molecule already shown in Figure 2b is also included.

keep the Rabi frequency Ω_R constant. The results (see Figure 3) are now also sensitive to the collection operator, as different physics arise if we examine the coherent case (obtained from the correlation function of the total dipole operator $\sum_{i=1}^N \hat{\sigma}_i$) or the incoherent sum over different molecules $\sum_i S_i(\omega)$, where $S_i(\omega) \propto \int_{-\infty}^{\infty} e^{i(\omega_L - \omega)\tau} \langle \hat{\sigma}_i^\dagger(\tau) \hat{\sigma}_i(0) \rangle$ is the Raman spectrum associated with one molecule. For coherent collection of the emission from the two molecules, the same spectral weight redistribution among the two polaritons (split by Ω_R , as in transmission measurements) is exhibited. By comparison with the case of a single molecule (also depicted in the figure), we infer a linear scaling proportional to N , which is consistent with the Λ -system results (eq 2). This confirms that no collective enhancement of the Raman signal is present. Interestingly, whereas, in a coherent collection, only the polaritons are observed in the spectrum, for an incoherent collection (which could be achieved experimentally using, e.g., a near-field probe), a central peak appears at the bare vibrational energy ω_v , a signature of the vibrational dark state

$$|d\rangle = \frac{1}{\sqrt{2}}(b_1^\dagger - b_2^\dagger)|G\rangle$$

This demonstrates that the dark-state emission is suppressed under coherent collection as a result of destructive interference (as observed within the Λ -system approach above), even though these states emit on the single-molecule level. Nonetheless, the total Raman signal $\int S(\omega) d\omega$ is almost independent of the collection method. Combined with the results above, we can thus conclude that, under strong coupling, the total dipole strength (proportional to N) is redistributed between the modes but not enhanced significantly.

In conclusion, we have investigated the effects of collective VSC in the Raman scattering of organic polymers. Using a series of increasingly complex models, we have demonstrated that the main effect of VSC is a redistribution of the total Raman cross section, with the Stokes lines for (multiple) vibrational excitation splitting into multiplets corresponding to (multiple) excitation of the lower and upper polaritons. The total cross section (integrated over the emission frequency) is approximately conserved. Using a simple analytical argument, we showed that this is true as long as the ultrastrong-coupling regime is not reached. Once the Rabi splitting becomes comparable to the transition frequency and ultrastrong coupling is achieved, the induced change in the ground state does lead to

an increase of the total integrated Raman cross section, with an enhancement by less than a factor of 2 for realistic values. We additionally found that the Stokes lines in the strongly coupled Raman spectrum are located at the same energies (and thus exhibit the same Rabi splitting) as in the transmission spectrum.

In contrast, a recent experiment⁹ found a large enhancement of the Raman signal by 2–3 orders of magnitude under VSC, as well as an increase in the Rabi splitting between the lower and upper polaritons by more than a factor of 2 in the Raman spectrum compared to the transmission spectrum. We thus finish by discussing additional effects that could affect Raman scattering under VSC and examine whether they can explain the discrepancy between theory and experiment.

First, in our models, we included only a single cavity mode, whereas a planar cavity supports a continuum of photonic modes. However, the argument based on eq 3 above does not depend on the number of cavity modes or molecules in the system. We additionally confirmed this by explicitly including multiple cavity modes within the three-level model (not shown). We also neglected the rotational degrees of freedom of the molecules. The counter-rotating coupling terms responsible for ultrastrong-coupling effects could lead to orientation of the molecules along the cavity-field polarization axis (if such an axis is well-defined). However, it was shown recently²³ that molecular orientation under strong coupling depends only on the single-molecule coupling strength without collective enhancement, such that this effect is negligible under realistic experimental conditions. Additionally, we did not consider that the molecular states could exhibit permanent dipole moments, which enable dipole transitions that do not change the state. We explicitly verified that including these transitions also does not lead to an increase of the integrated Raman cross section under strong coupling.

One remaining possibility for explaining the increased Raman yield observed in the experiments within linear response is that an (unknown) VSC-induced process could lead to a modification of the bare-molecule dipole transition strengths. This would require an increase by a factor of about $(1000)^{1/4} \approx 6$ for each of the dipole moments, μ_{ge} and μ_{ev} . This change is not contained within the state modifications induced by ultrastrong coupling that are fully incorporated in our modeling. Nevertheless, the increase in the dipole strengths would not provide an explanation for the increased Rabi splitting observed in Raman versus transmission spectra.

Finally, we have up to now neglected nonlinear effects and calculated only the linear response of Raman scattering. Typically, Raman cross sections are quite small, and nonlinear effects are thus negligible under weak coupling. However, under strong coupling, the number of populated final states reached by Raman scattering is dramatically reduced, from (within the first Stokes line) one per molecule to just two extended polaritons. If the effective polariton excitation rate becomes higher than its lifetime, this could lead to an accumulation of polaritons and, subsequently, bosonic enhancement of the Raman scattering. These nonlinear interactions could also induce polariton energy shifts, such that nonlinear behavior could possibly explain both the experimentally observed enhancement as well as energy shift under Raman scattering. Although a more detailed treatment is beyond the scope of this article, it should be noted that order-of-magnitude estimates indicate that, in the experiments,⁹ excitations are created significantly more slowly than the polariton decay rate. Therefore,

nonlinear behavior would be expected only if there were an additional enhancement factor in the system independent of strong coupling (such as the presence of local field enhancement at hot spots if the mirror surfaces have a rough structure). This highlights the necessity for further theoretical and experimental exploration of nonlinear effects in Raman scattering processes under vibrational strong coupling.

AUTHOR INFORMATION

Corresponding Authors

*E-mail: francisco.delpino@uam.es (J.d.P.).

*E-mail: johannes.feist@uam.es (J.F.).

*E-mail: fj.garcia@uam.es (F.J.G.-V.).

Notes

The authors declare no competing financial interest.

ACKNOWLEDGMENTS

We thank A. Shalabney and T. Ebbesen for helpful discussions. This work was funded by the European Research Council (ERC-2011-AdG Proposal 290981), the European Union Seventh Framework Programme under Grant Agreement FP7-PEOPLE-2013-CIG-618229, and the Spanish MINECO under Contract MAT2014-53432-C5-5-R.

REFERENCES

- (1) Colthup, N. B.; Daly, L. H.; Wiberley, S. E. *Introduction to Infrared and Raman Spectroscopy*; Academic Press: San Diego, CA, 1990.
- (2) Shalabney, A.; George, J.; Hutchison, J.; Pupillo, G.; Genet, C.; Ebbesen, T. W. Coherent coupling of molecular resonators with a microcavity mode. *Nat. Commun.* **2015**, *6*, 5981.
- (3) Long, J. P.; Simpkins, B. S. Coherent Coupling between a Molecular Vibration and Fabry-Perot Optical Cavity to Give Hybridized States in the Strong Coupling Limit. *ACS Photonics* **2015**, *2*, 130–136.
- (4) George, J.; Wang, S.; Chervy, T.; Canaguier-Durand, A.; Schaeffer, G.; Lehn, J.-M.; Hutchison, J. A.; Genet, C.; Ebbesen, T. W. Ultra-strong coupling of molecular materials: spectroscopy and dynamics. *Faraday Discuss.* **2015**, *178*, 281–294.
- (5) del Pino, J.; Feist, J.; Garcia-Vidal, F. J. Quantum theory of collective strong coupling of molecular vibrations with a microcavity mode. *New J. Phys.* **2015**, *17*, 053040.
- (6) Simpkins, B. S.; Fears, K. P.; Dressick, W. J.; Spann, B. T.; Dunkelberger, A. D.; Owrutsky, J. C. Spanning Strong to Weak Normal Mode Coupling between Vibrational and Fabry-Pérot Cavity Modes through Tuning of Vibrational Absorption Strength. *ACS Photonics* **2015**, *2*, 1460–1467.
- (7) Carusotto, I.; Ciuti, C. Quantum fluids of light. *Rev. Mod. Phys.* **2013**, *85*, 299–366.
- (8) Törmä, P.; Barnes, W. L. Strong coupling between surface plasmon polaritons and emitters: a review. *Rep. Prog. Phys.* **2015**, *78*, 013901.
- (9) Shalabney, A.; George, J.; Hiura, H.; Hutchison, J. A.; Genet, C.; Hellwig, P.; Ebbesen, T. W. Enhanced Raman Scattering from Vibro-Polariton Hybrid States. *Angew. Chem., Int. Ed.* **2015**, *54*, 7971–7975.
- (10) Nie, S.; Emory, S. R. Probing Single Molecules and Single Nanoparticles by Surface-Enhanced Raman Scattering. *Science* **1997**, *275*, 1102–1106.
- (11) Campion, A.; Kambhampati, P. Surface-enhanced Raman scattering. *Chem. Soc. Rev.* **1998**, *27*, 241–250.
- (12) Kneipp, J.; Kneipp, H.; Kneipp, K. SERS - a single-molecule and nanoscale tool for bioanalytics. *Chem. Soc. Rev.* **2008**, *37*, 1052–1060.
- (13) Roelli, P.; Galland, C.; Piro, N.; Kippenberg, T. J. Molecular cavity optomechanics as a theory of plasmon-enhanced Raman scattering. *Nat. Nanotechnol.* **2015**, DOI: 10.1038/nnano.2015.264.

- (14) Kosztin, J.; Zawadowski, A. Violation of the f-sum rule for Raman scattering in metals. *Solid State Commun.* **1991**, *78*, 1029–1032.
- (15) Freericks, J. K.; Devereaux, T. P.; Moraghebi, M.; Cooper, S. L. Optical Sum Rules that Relate to the Potential Energy of Strongly Correlated Systems. *Phys. Rev. Lett.* **2005**, *94*, 216401.
- (16) de'Medici, L.; Georges, A.; Kotliar, G. Sum-rules for Raman scattering off strongly correlated electron systems. *Phys. Rev. B: Condens. Matter Mater. Phys.* **2008**, *77*, 245128.
- (17) Ciuti, C.; Bastard, G.; Carusotto, I. Quantum vacuum properties of the intersubband cavity polariton field. *Phys. Rev. B: Condens. Matter Mater. Phys.* **2005**, *72*, 115303.
- (18) Casanova, J.; Romero, G.; Lizuain, I.; García-Ripoll, J. J.; Solano, E. Deep Strong Coupling Regime of the Jaynes-Cummings Model. *Phys. Rev. Lett.* **2010**, *105*, 263603.
- (19) Niemczyk, T.; Deppe, F.; Huebl, H.; Menzel, E. P.; Hocke, F.; Schwarz, M. J.; Garcia-Ripoll, J. J.; Zueco, D.; Hümmer, T.; Solano, E.; Marx, A.; Gross, R. Circuit quantum electrodynamics in the ultrastrong-coupling regime. *Nat. Phys.* **2010**, *6*, 772–776.
- (20) Todorov, Y.; Andrews, A. M.; Colombelli, R.; De Liberato, S.; Ciuti, C.; Klang, P.; Strasser, G.; Sirtori, C. Ultrastrong Light-Matter Coupling Regime with Polariton Dots. *Phys. Rev. Lett.* **2010**, *105*, 196402.
- (21) Schwartz, T.; Hutchison, J. A.; Genet, C.; Ebbesen, T. W. Reversible Switching of Ultrastrong Light-Molecule Coupling. *Phys. Rev. Lett.* **2011**, *106*, 196405.
- (22) Galego, J.; Garcia-Vidal, F. J.; Feist, J. Cavity-Induced Modifications of Molecular Structure in the Strong-Coupling Regime. *Phys. Rev. X* **2015**, *5*, 041022.
- (23) Ćwik, J. A.; Kirton, P.; De Liberato, S.; Keeling, J. Self-consistent molecular adaptation induced by strong coupling. 2015, arXiv.org e-Print archive. <http://arxiv.org/abs/1506.08974>.
- (24) Breuer, H.-P.; Petruccione, F. *The Theory of Open Quantum Systems*; Oxford University Press: Oxford, U.K., 2007.
- (25) Wangsness, R. K.; Bloch, F. The Dynamical Theory of Nuclear Induction. *Phys. Rev.* **1953**, *89*, 728–739.
- (26) Redfield, A. G. Nuclear magnetic resonance saturation and rotary saturation in solids. *Phys. Rev.* **1955**, *98*, 1787–1809.
- (27) Johansson, J. R.; Nation, P. D.; Nori, F. QuTiP 2: A Python framework for the dynamics of open quantum systems. *Comput. Phys. Commun.* **2013**, *184*, 1234–1240.